International Journal of Electrical, Electronic and Communication Sciences
ISSN: 2517-9438
Vol:10, No:12, 2016

Experimental Analyses of Thermoelectric Generator Behavior Using Two Types of Thermoelectric Modules for Marine Application

A. Nour Eddine, D. Chalet, L. Aixala, P. Chessé, X. Faure, N. Hatat

***Abstract*—**Thermal power technology such as the TEG (Thermo-Electric Generator) arouses significant attention worldwide for waste heat recovery. Despite the potential benefits of marine application due to the permanent heat sink from sea water, no significant studies on this application were to be found. In this study, a test rig has been designed and built to test the performance of the TEG on engine operating points. The TEG device is built from commercially available materials for the sake of possible economical application. Two types of commercial TEM (thermo electric module) have been studied separately on the test rig. The engine data were extracted from a commercial Diesel engine since it shares the same principle in terms of engine efficiency and exhaust with the marine Diesel engine. An open circuit water cooling system is used to replicate the sea water cold source. The characterization tests showed that the silicium-germanium alloys TEM proved a remarkable reliability on all engine operating points, with no significant deterioration of performance even under sever variation in the hot source conditions. The performance of the bismuth-telluride alloys was 100% better than the first type of TEM but it showed a deterioration in power generation when the air temperature exceeds 300 °C. The temperature distribution on the heat exchange surfaces revealed no useful combination of these two types of TEM with this tube length, since the surface temperature difference between both ends is no more than 10 °C. This study exposed the perspective of use of TEG technology for marine engine exhaust heat recovery. Although the results suggested non-sufficient power generation from the low cost commercial TEM used, it provides valuable information about TEG device optimization, including the design of heat exchanger and the types of thermo-electric materials.

***Keywords*—**Internal combustion engine application, Seebeck, thermo-electricity, waste heat recovery.

I. Introduction

AROUND 55-60% of the fuel energy supplied to internal combustion engine is wasted as heat in the exhaust and cooling systems [1], [2]. In this context, recycling and reusing waste exhaust gas cannot only enhance fuel energy use efficiency, but also reduce air pollution.

A. Nour Eddine is with the commissariat of atomic and alternative energies – district of Pays de la Loire, Bouguenais, 44340 France (corresponding author to provide phone: 0033781880797; e-mail: ali.noureddine@ cea.fr).

D. Chalet and P. Chessé are with Ecole Centrale de Nantes, LHEEA lab. (ECN/CNRS), Nantes, 44300 France (e-mail: david.chalet@ec-nantes.fr, pascal.chesse@ec-nantes.fr).

L. Aixala is with the commissariat of atomic and alternative energies, laboratory of thermoelectricity, Grenoble, 38000 France (e-mail: luc.aixala@cea.fr).

X. Faure and N. Hatat are with the commissariat of atomic and alternative energies – district of Pays de la Loire, Bouguenais, 44340 France (e-mail: xavier.faure@cea.fr, Nicolas.hatat@cea.fr).

Among several waste heat recovery technologies such as turbo-compound [3], bottoming cycles [4], [5], and turbocharger [6], thermal power technology such as the thermoelectric generator (TEG) arouses significant attention worldwide. TEG is a technology for direct conversion of thermal energy into electrical energy, which has the merits to be reliable (no moving parts), quiet in operation, compact, and emission-less [7]. Previous studies have estimated that an increase of 10% of fuel efficiency can be easily achieved by converting about 6% of the waste heat into electricity [8], although some other publications indicate a more realistic gain of 2-3% [9].

The Seebeck effect, discovered by Thomas Johann Seebeck in 1821, is the fundamental operating principle of TEG [10]. The energy conversion efficiency of TE devices is measured by the figure of merit (ZT). Commercial TE materials with ZT>1 are not available; thus, the conversion efficiency of current TE materials is less than 5% [11]. Te-based alloys in combination with Bismuth (Bi), Antimony (Sb), or Selenium (Se) are referred to as low temperature materials (up to 300 °C), although lead tellurium could be used until far higher temperature. Currently, research efforts are focused on finding efficient, non-costly, and environmental friendly thermoelectric materials for energy conversion. Silicides, skutterudites, Sulfides, and half-Heusler materials are very promising candidates, and silicon-germanium (SiGe) alloys can be operated at the highest temperatures, up to 1100 °C [12]. Moreover, in order to achieve the highest average ZT over the entire operating temperature range of exhaust gases, different thermoelectric elements could be employed [13].

Since 1914, the possibility of using thermoelectric power generation to recover some of waste heat energy from reciprocating engines has been explored and patented [14], and with the development of novel TE materials, researchers have paid significant attention in this area over the last 20 years. Zhang et al. [15] studied the best position of the TEG considering the temperature distribution of the exhaust gas system of diesel engine. Yu et al. [16] optimized the TEG output by installing a power conditioning system between the TEG and the battery pack. Hsu et al. [17] used slopping block to uniform the thermal distribution in a three-row heat exchanger which improved the performance of the TEG. Kim et al. [18] developed a TEG system with the engine coolant of light-duty vehicles as heat source, and the output power was about 75 W. In his study, the conventional radiators of the existing water cooling system were replaced by the TEG

system [19], [20].

The previous studies for exhaust heat recovery by TEG mainly focused on automotive applications; however, the employment of this technology for marine application is far more interesting. On one hand, the marine Diesel engines reach around 400-450 °C at turbocharger exhaust, corresponding to 200-300 °C of hot side thermoelectric module (TEM) temperature, which is interesting according to the recent studies on intermediate temperatures TE materials [21]. In addition, seawater is available in abundance and is an excellent heat sink. On the other hand, the engine fuel consumption is a major factor on ship operational costs; hence, a slight reduction of fuel consumption generates significant financial savings.

In this study, operating points from a Diesel engine are simulated on a test bench. The behavior and performance of two commercial TE materials is investigated by using an automotive grade heat exchanger. The conversion efficiency is measured and scaled to predict the performance in marine application. For this purpose, a model to quantify the wasted heat recovery is developed.

II. TEG Description

A waste heat recovery thermoelectric conversion system normally consists of TEM, heat absorbers, and heat sinks, where heat is transferred from a high-temperature heat source to the TEM hot junction, and it is rejected to a low-temperature sink from the TEM cold junction. Based on the Seebeck effect, the heat supplied at the hot junction causes an electric current flow in the circuit, and electrical power is produced. The Seebeck effect is generally dominated by the contribution from charge carrier diffusion which tends to push charge carriers towards the cold side of the material until a compensating voltage has built up. As a result, in p-type semiconductors, α is positive. Likewise, in n-type semiconductors, α is negative. In most conductors, however, the charge carriers exhibit both hole-like and electron-like behavior and the sign of α usually depends on the predominating one. The current flow through the Thermo-Electric Module can be determined by:

$$I = \alpha \Delta T/(R_I + R_L) \quad (1)$$

where $\alpha(V.K^{-1})$ is the Seebeck coefficient, $R_I(\Omega)$ is the internal resistance of the thermoelectric generator, and $R_L(\Omega)$ is the load resistance. The heat flow to the hot side and heat flow out of the cold side can be written as:

$$Q_h = K\Delta T + \alpha T_h I - 1/2\, I^2 R_I \quad (2)$$

$$Q_c = K\Delta T + \alpha T_c I - 1/2\, I^2 R_I \quad (3)$$

where K consists of many parts of thermal conductance and thermal resistance. The produced power can be expressed in two different ways, either by the difference of heat going in and coming out equations or by applying the Ohm law equation. A figure of merit, Z, is used to define the performance of a thermoelectric material. It is derived from the Seebeck coefficient $\alpha(V.K^{-1})$, electrical conductivity $\sigma(Siemens.m^{-1})$, and thermal conductivity $\lambda(W.m^{-1}.K^{-1})$ of the material:

$$Z = \alpha^2 \sigma / \lambda \quad (4)$$

The product ZT, where $T = (T_h + T_c)/2$, is a non-dimensional number that expresses the figure of merit under a given working temperature. The maximum thermal efficiency is directly dependent on the figure of merit and the difference of temperature between the hot (T_h) and cold (T_c) junctions:

$$\eta_{max} = \left[\frac{\sqrt{(1 + \overline{ZT})} - 1}{\sqrt{(1 + \overline{ZT})} - 1 + \frac{T_c}{T_h}} \right] \left[\frac{T_h - T_c}{T_h} \right] \quad (5)$$

At the point of maximum thermal efficiency, the load resistance should be related to the internal resistance of the thermoelectric generator as:

$$R_L/R_I = \sqrt{(1 + \overline{ZT})} \quad (6)$$

A TE couple is constituted from n-type and p-type semiconductor thermoelectric legs (e.g. silicon-germanium SiGe, bismuth-telluride BiTe based alloys) which are sandwiched between ceramic plates and configured thermally in parallel and electrically in series. The junctions connecting the thermoelectric legs between the hot and cold plates are generally using highly conducting metal (e.g. Copper, Nickel, Silver). More than one pair of TE couple are normally assembled together to form TEM.

In this study, a single tube automotive grade TEG device provided by HotBlock OnBoard (HBOB) is used. For the sake of building a TEG from commercially available materials, two types of TEM have been chosen (Table I).

A. Thermoelectric Modules

A MAN Diesel & Turbo marine Diesel engine was selected for the input conditions of this work, and a typical range of exhaust temperature and flow values were given by the company [22]. The exhaust gas temperatures on (5-25 MW) marine Diesel engines can reach up to 550 °C at the turbine outlet. However, the slow steaming mode [23], which is representative of the large ships operating points, is corresponding to 300-400 °C at the turbine outlet. Hence, the most compatible materials for Diesel engine applications are intermediate temperatures TEM. Few TEM suppliers are currently able to sell small dimensions (less than 25 cm^2) and reliable TEM with skutterudites, magnesium-silicon, of half-Heusler alloys, at least at a competitive price. Those, using Bi-Te TEM for low charge operating points of marine engine and SiGe alloys TEM for the other operating points were the most interesting solutions for our study. Our choice fell on the module TECB-79-165 from CIDETE Ingenieros SL for the

Bi_2Te_3. It delivers 2.5 W of maximum power (for a ΔT=200 °C), and can resist up to 219 °C. Our second choice fell on a $Si_{80}Ge_{20}$ based TEM developed for energy recovery from the thermal sources above 450 °C. Knowing that it is not the best compatible with engine exhaust temperatures (550 °C max), it was chosen because it showed a particular stability (this material was used for radioisotope thermoelectric generator (RTG) in satellites and space probes applications) and interesting performances (Figure of merit around 0.5 at 500-600 °C). The $Si_{80}Ge_{20}$ based TEM called NEMO [24] from HBOB SAS has a heat exchange surface of 20 mm x 20 mm. It delivers a maximum power of 3.7 W (for a ΔT=500 °C). Although it contains germanium (a costly element), literature is showing some interesting studies which reduce the Ge content to a low percentage in order to lower its cost [25]. Figs. 1 and 2 show the difference in performance and operating temperatures between the two types of TEM. The figure of merit of these specific modules from the supplier data sheet are compared with the best known performance that exists in the literature [26].

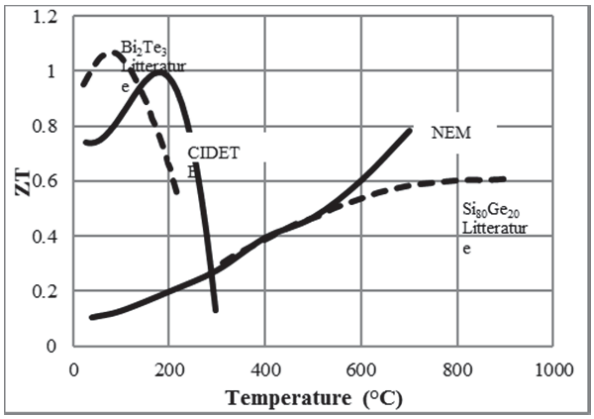

Fig. 1 Figure of merit for p-type thermoelectric materials

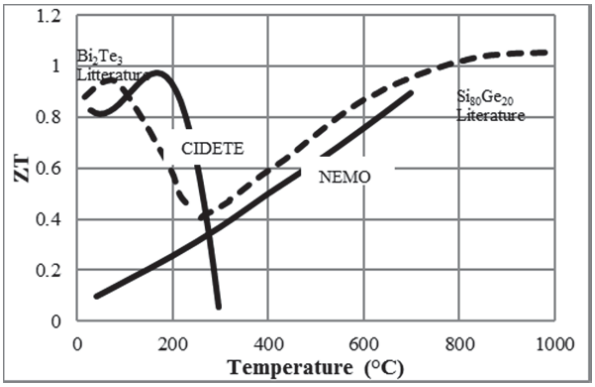

Fig. 2 Figure of merit for n-type thermoelectric materials

B. Thermoelectric Generation Device

Fig. 3 shows a description of the TEG device. The hot side heat exchanger is composed of a stainless steel tube with internal fins. The tube is mounted between two flanges. The connection of the tube to the air circuit is made by the intermediate of a divergent and a convergent manifold. Each of them is mounted on a flange, screwed to the tube flange, and sealed with graphite joint. The tube is of "plate & fin" type in terms of architecture and to the "flat tube & fin" in terms of heat exchange. The inner fins are of "wavy" design, and the thickness of heat exchange surface is 1 mm. 270 µm grooves were formed on the heat exchange surface in order to insert 250 µm (type K) thermocouples, for measuring the accurate hot side temperature without affecting the thermal contact between the TEM and the heat exchange surface.

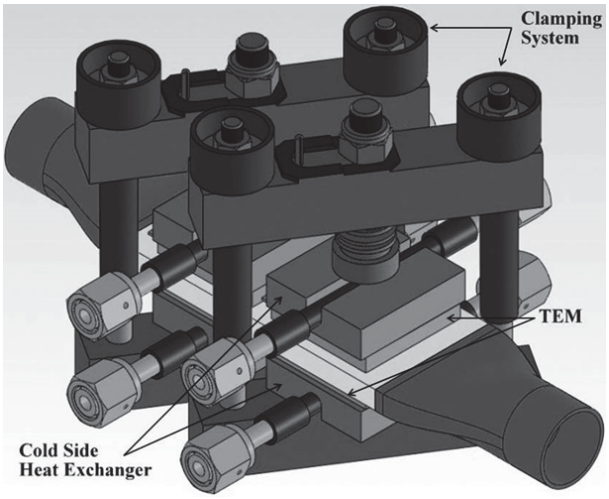

Fig. 3 The thermoelectric conversion device used (courtesy of HBOB SAS and CEA Tech)

The cold side heat exchanger is composed of two cold plates, ensuring the cooling of the TEM positioned on the lower and upper side of the tube. The cooling is achieved by circulating water in a ¼ inch copper tubing network. The heat is then transmitted to the TEM via aluminum brazed thermal spreaders, around the copper pipes. Each TEM is individually cooled by a spreader to ensure the best possible thermal contact. Each spreader is provided with an imprint on its outside surface to ensure its coupling with the clamping system.

The clamping system is individual for each column. It consists of two plates outfitted with threaded rod, spring, and nut, allowing to apply individual compressive stress of 17.85 MPa on each TEM on the two sides of the hot side heat exchanger. Hence, its main objective is to ensure good thermal contact between the TEM and the heat exchangers.

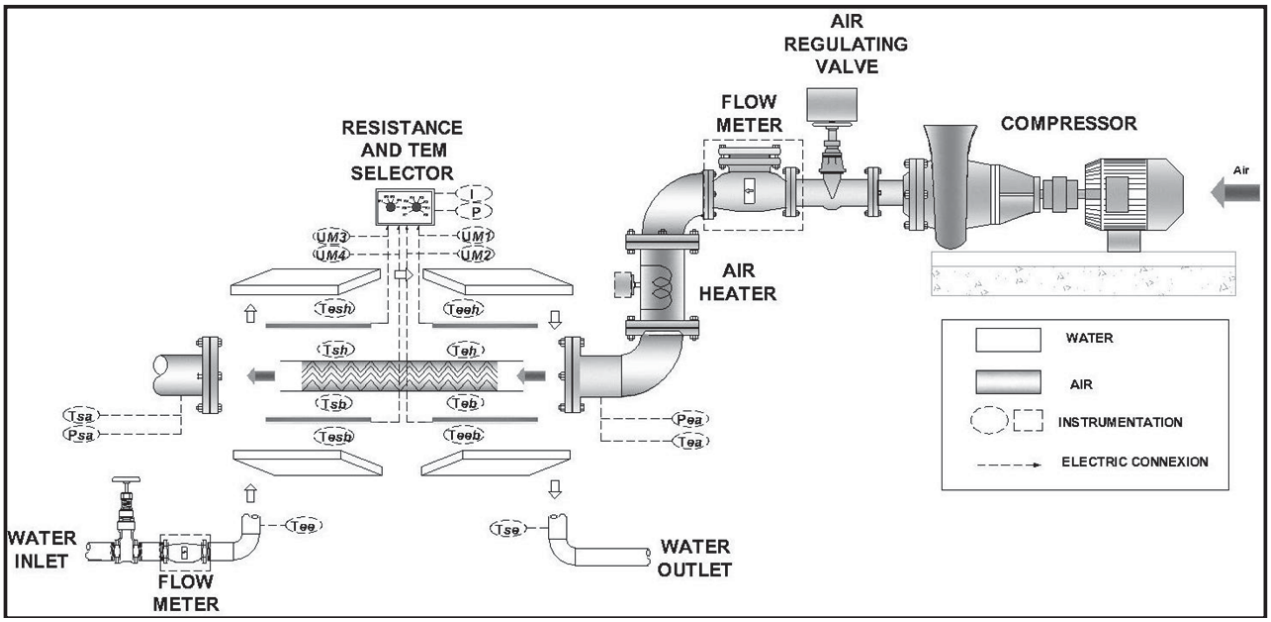

Fig. 4 Schematic diagram of the experimental set-up for the steady state condition

TABLE I
THERMOELECTRIC MODULES PROPERTIES (SUPPLIER INFORMATION)

	CIDETE Ingenieros	HotBlock OnBoard
Thermoelectric material type	Bi_2Te_3	$Si_{80}Ge_{20}$
Physical Properties		
Dimensions, mm	20 ± 0.1×20 ± 0.1 ×3.8 ± 0.01	20 ± 0.5×24 ± 0.5 ×7.1± 0.05
Flatness, mm	0.02	0.02
Thickness tolerance, mm	0.02	0.05
Number of active couples, pcs	71	12
Thermal Properties		
Design Hot Side Temperature, °C	220	580
Design Cold Side Temperature, °C	20	80
Thermal conductivity, W/K	0.26	0.53
Heat Flux, W	52	
Electric Properties		
Power, W	2.45	3.6 ± 6%
Internal Resistance, Ohm	2.80	0.48 ± 6%
Current, A	0.98	5.53 ± 5%
Opened Circuit Voltage, V	5.00	2.6 ± 5%
Efficiency, %	3.7	2.6

III. EXPERIMENTAL TEST RIG AND PROCEDURES

In this study, the power characteristics and behavior of the TEG on engine operating points were investigated by using a hot air rig tests. The tests were held under steady state conditions (the gas flow was purified from impulsive flow). The air temperature and the flow rate were the variables representing engine operating points. The experimental setup of the test rig is shown in Fig. 4. The air supply for simulating the engine exhaust gas was provided by two air compressors in parallel. The first is a 75 kW variable speed compressor (MAVD 1000). The second is a 45 kW compressor (MAVD 700). The compressed air was stored in a tank to ensure a steady and pulse-free supply. The air flow was transferred to a dryer and filter to remove water and impurities and an electric regulating valve (PSL204AMS) was used to control the air flow. A 144 kW electric heater (Osram-Sylvania) is then used to increase the temperature of the air which was guided to the single tube heat exchanger.

A. Instrumentation

The control of the different parameters is made through Labview® outside the test rig room. The regulating valve is controlled by using opening percentage, then the flow rate is measured with a flow meter located downstream the valve. The minimum opening required for air to circulate is 25% leading to a minimum airflow of 11 g/s. Furthermore, the temperature losses in the air circuit have limited the air temperature at a maximum of 485 °C on the inlet of the hot side heat exchanger. An open circuit (the potential type of circuit designed for marine application) water tubing was used as the heat sink. The city water (temperature ranging from 20 to 24 °C) is used to feed the cooling system. The flow is maintained constant at 20 g/s by using a gate valve. A flow meter located downstream of the gate valve measured the flow rate of the water which was guided afterward to simultaneously feed the four cold heat exchangers.

Table II represents the sensors installed on the test rig. The hot side and cold side temperatures as well as the generated voltage and currents were measured for each TEM. Four types of K with 250 µm diameters thermocouples were placed between the external surface of the single tube heat exchanger and the TEM via micro-grooves on the tube external shell to measure the hot side temperature. For the cold side temperature, four, type K with 1 mm diameters thermocouples were placed between the external surface of the cold side heat

exchanger and the TEM via micro-grooves. Measurements were also made upstream and downstream the single tube heat exchanger to obtain precisely the input/output air pressures and temperatures. The pressure losses through the heat exchanger and the dissipated heat through the heat exchanger are then evaluated. 1.5 mm type K thermocouples were as well installed on the inlet and outlet of the cooling system to ensure constant temperature on water inlet and evaluate the heat dissipated through the cooling system.

TABLE II
TEST RIG INSTRUMENTATION

Symbol	Instrumentation
Tse	Water outlet temperature
Tee	Water inlet temperature
Tea	Air inlet temperature
Tsa	Air outlet temperature
Tesb	Cold side TEM temperature (position low left)
Teeb	Cold side TEM temperature (position low right)
Tesh	Cold side TEM temperature (position high right)
Teeh	Cold side TEM temperature (position high left)
Teb	Hot side TEM temperature (position low right)
Tsb	Hot side TEM temperature (position low left)
Teh	Hot side TEM temperature (position high right)
Tsh	Hot side TEM temperature (position high left)
Pea	Air inlet pressure
Psa	Air outlet pressure
UM1	TEM 1 voltage
UM2	TEM 2 voltage
UM3	TEM 3 voltage
UM4	TEM 4 voltage
P	Generated power
I	Generated current

The generated voltage and power were recorded by using a NI MAX data acquisition system. Two rotary manual selectors were used for the TEM and load resistance variation. The TEM were connected separately to the load resistance and the data acquisition box. It allows isolating the effect of a malfunctioning TEM during the essays.

B. Tests Protocol

The tests were conducted by using the engine operating points to evaluate the performance of the Bi_2Te_3 and $Si_{80}Ge_{20}$ TEM integrated in a TEG device. The engine used as a reference for the study was a commercial automotive Diesel engine with a displacement of 1.5 L, and its specifications are presented in Table III. The engine data sheet was used to characterize its operating points. The flow rate and temperature of the engine exhaust gas on each operating points were replicated on the hot air test rig. During the tests, the flow rate and the temperature of the water remained constant. Only the effects of temperature and flow rate variations of the hot air were studied. The characterization of the $Si_{80}Ge_{20}$ TEM was limited to 56 engine operating points due logistic constraints (maximum reachable temperature 485 °C, maximum reachable flow 43 g/s). The characterization of the Bi_2Te_3 TEM was limited to 36 engine operating points due to safety constraints due to telluride toxic emissions above 400 °C, although the safety temperature specified by the supplier for guaranteed performance is limited to 219 °C. An example of 5 engine operating point's characteristics and test rig conditions is presented in Table IV.

TABLE III
ENGINE SPECIFICATIONS USED FOR THE TEST RIG

Model	Diesel engine
Displacement	1461 cm^3
Cylinder bore	76 mm
Piston stroke	80.5 mm
Compression ratio	15.2:1
Maximum power (hp)	68 at 4000 r/min
Maximum torque (N.m)	200 at 2000 r/min

TABLE IV
EXAMPLE OF TEST RESULTS ON THE HOT AIR RIG FOR 5 POINTS

Engine operating points				Tests rig	
Speed (r/min)	Torque (N.m)	Turbine outlet Temperature (°C)	Exhaust gas flow rate (g/s)	Air temperature (°C)	Air flow rate (g/s)
1000	45	243.7	13.88	244	13.9
1250	0	129.3	16.4	129	16.4
1500	15	167.5	18.1	168	18
1750	40	276.4	21.19	276	21.2
2500	75	358.29	45.19	358	45

The TEMs were connected independently to an external variable resistor load, and the output voltage was measured via data acquisition box. Flexible copper wires were used for the connections between the TEM and the variable load resistor. Power generated by the TEM can be calculated by using the voltage and resistor values. All data readings for computer processing were made at thermal equilibrium condition, when temperature fluctuation was less than 1°C over 5 min. The variation of the load resistor and TEM selector was made manually as shown in Fig. 5.

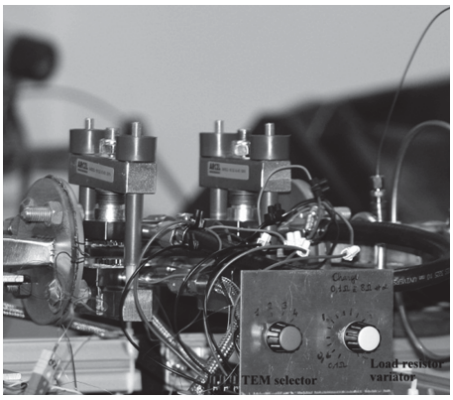

Fig. 5 Photograph of the TEG device equipped with manual load and TEM selector

The main target of the experiment was generated power and TEG efficiency. The generated power was measured by using voltage values with resistors of different values connected in series to the external circuit. Four values of resistors were tested over the experiment (R_1= 7.87 Ω, R_2=3.87 Ω, R_3= 1.52

Ω and R_4= 0.2 Ω). These values represent the boundary conditions of internal resistance variations with temperature since the maximum power mode is considered when the load resistance is equal to the TEM internal resistance. The calculation of these values took into consideration the data sheet of the TEM provided by the manufacturer and the electrical resistance of the electrical wires. While the electrical resistance of the wires had no remarkable influence on the load resistance calculation for the Bi_2Te_3 TEM since it represents between 0.08 and 0.1% of the TEM internal resistance, it was taken into consideration for the $Si_{80}Ge_{20}$ load resistance calculation since it represents between 1 and 2% of the TEM internal resistance. The TEG total generated power was calculated by adding the power generated by each TEM loaded simultaneously and not by connecting the TEM in series and applying the load resistance. This assumption for the total generated power was used for the calculation of the TEG efficiency.

IV. Results and Discussions

Two test campaigns were carried out on the test rig to determine whether one or both of these TEMs can be applied in a real engine. These two tests shared the same heat exchanger, dimensions, the same number of TEMs, and same cooling and clamping system. Fig. 6 shows the hot and cold side temperatures of the TEM positioned on the inlet and outlet of the heat exchanger according to the air inlet temperatures. As can be seen from Fig. 6, the temperature from inlet air temperatures (corresponding to the turbine outlet temperature in a Diesel engine) was measured from around 108 °C to a maximum of around 485 °C. On the other hand, the temperature on the heat exchange surface between the hot side heat exchanger and the TEM placed on the exhaust gas inlet was measured from around 82 °C to a maximum of around 468 °C which is different than reported values in literature as it will be discussed later, due to sonic nozzle in the heat exchanger. This temperature was 3 – 8 °C higher than the hot side temperature of the TEM placed on the exhaust gas outlet. This gap tends to increase with increasing the air inlet temperature.

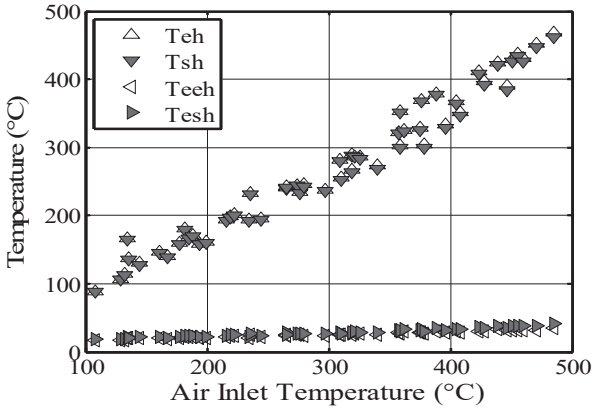

Fig. 6 Air inlet temperature (°C) *vs.* TEM hot and cold side temperature (°C)

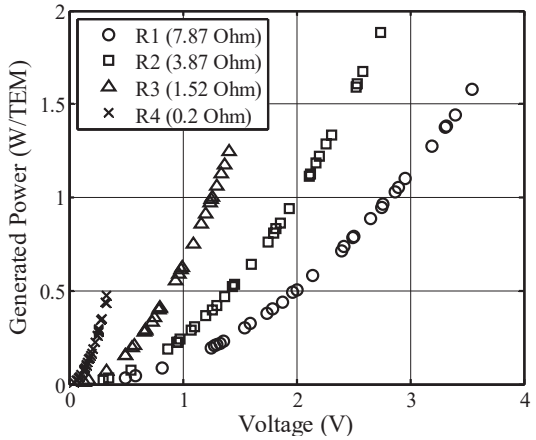

Fig. 7 Bi_2Te_3: output voltage (V) *vs.* TEM Generated power (W)

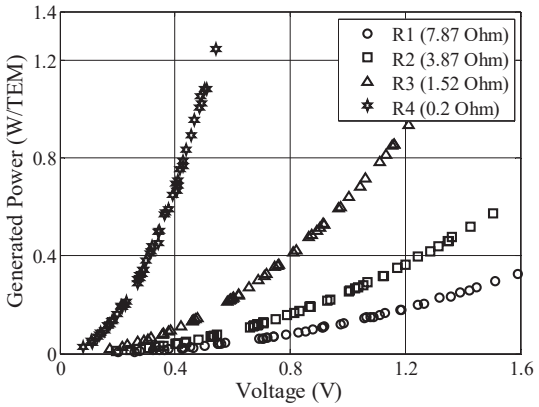

Fig. 8 $Si_{80}Ge_{20}$: output voltage (V) *vs.* TEM Generated power (W)

The temperature of the heat exchange surface between the cold side heat exchanger and the TEM placed on the air inlet was measured from around 17 °C to a maximum of 40 °C for a water inlet temperature of 15 °C. The temperature difference between this last and the one corresponding to the TEM place on air outlet was less than 1 °C, which is more than the uncertainty of the thermocouples installed. This leads a difference between the hot and cold sides temperature of the TEM from around 65 °C to 430 °C.

Figs. 7 and 8 show the generated power (P) of Bi_2Te_3 and $Si_{80}Ge_{20}$ modules according to the generated voltage (V). The voltage has tendencies to increase with increasing the load resistance (R) in both TEM. For Bi_2Te_3 modules the maximum TEG generation power output is achieved when the load resistance is equal to 3.87 Ω. Hence for the $Si_{80}Ge_{20}$ modules, it is achieved when the load resistance is equal to 0.2 Ω. The present result agrees with the maximum power transfer theory. The maximum power conversion occurs when the load resistor equals the internal resistance, which is in this case 2-3 Ω for the Bi_2Te_3 TEM and 0.03-0.13 for the $Si_{80}Ge_{20}$ TEM. The generated power is obtained by using (7) which justifies the hyperbolic shape of the curve.

$$P = U^2 / R \quad (7)$$

Figs. 9 and 10 show the performances of the thermoelectric module according to the TEM hot side temperature. Since each engine operating point has different temperature and flow rate, it was not possible to represent the performance according to the temperature of the high temperature source obtained from rig test device.

During the tests, the flow and temperature of the water were maintained constant, so the low temperature source has nearly no effect on the temperature difference between the hot and cold side of the module. As can be seen from the figures, when the difference between the high temperature source and the low temperature source increased, the power increased. This characteristic is obtained when the electricity is generated by a temperature difference in a thermoelectric element. A maximum output of 1.9 W was achieved by the Bi_2Te_3 module for TEM hot side temperature around 312 °C corresponding to air inlet temperature of 362 °C. During the tests, the performance of the Bi_2Te_3 modules was greatly impaired when the TEM hot side temperature exceeded 210 °C. Furthermore, the performances of some modules deteriorated in comparison with those seen on the same temperature range before exceeding this temperature. This might have been caused by durability issues (brazing damage). The actual allowable safety temperature of Bi2Te3 TEM used in this study is around 219 °C (as indicated by CIDETE Ingenieros SL in the product description), but Bi_2Te_3 TEMs with higher operating temperature are also available [27] (320 °C in continuous operation), although the maximum temperature without TEM encapsulation has always to be limited to around 400 °C due to possible toxic gas formation. However, for engine operating points case, since the temperature of the exhaust gas under most loads is higher than 210 °C, we exceeded the allowable temperature which may have gradually impaired the performance of Bi_2Te_3 TEM.

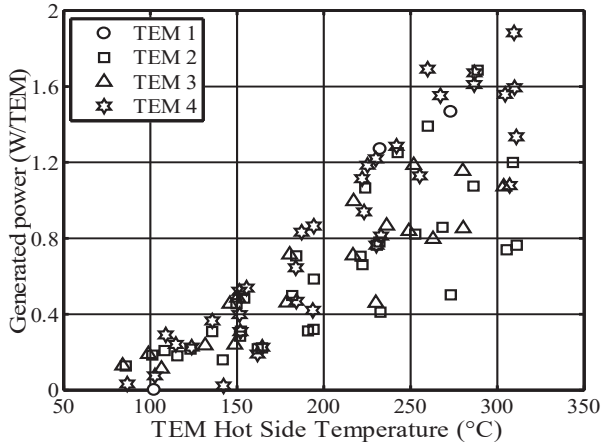

Fig. 9 Bi_2Te_3: TEM hot side temperature (°C) *vs.* TEM Generated power (W) on maximum power mode

The $Si_{80}Ge_{20}$ TEM showed remarkable stability throughout the test. A maximum power output of 1.3 W was achieved for an inlet air temperature of 485 °C and a flow rate of 43 g/s. The power produced by the $Si_{80}Ge_{20}$ TEM is lower than that produced by the Bi_2Te_3 TEM as shown in Fig. 11, which is normal since the optimal performance of the $Si_{80}Ge_{20}$ TEM is reached for a hot side temperature of around 800 °C, corresponding to air temperature of 900 °C. As it is clearly illustrated in Fig. 11, the $Si_{80}Ge_{20}$ modules may not have the best performance on these engine operating points, but it can get us further in the tests to provide stable performance on all engine operating points.

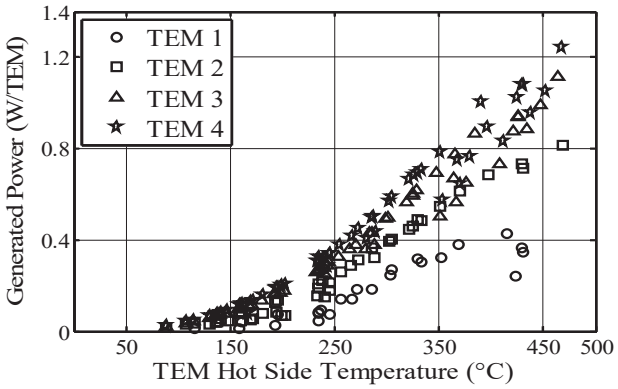

Fig. 10 $Si_{80}Ge_{20}$: TEM hot side temperature (°C) vs. TEM Generated power (W) on maximum power mode

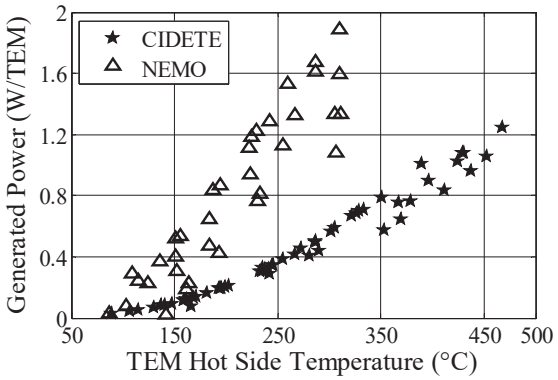

Fig. 11 Bi_2Te_3 *vs.* $Si_{80}Ge_{20}$: TEM hot side temperature (°C) vs. TEM Generated power (W) on maximum power mode

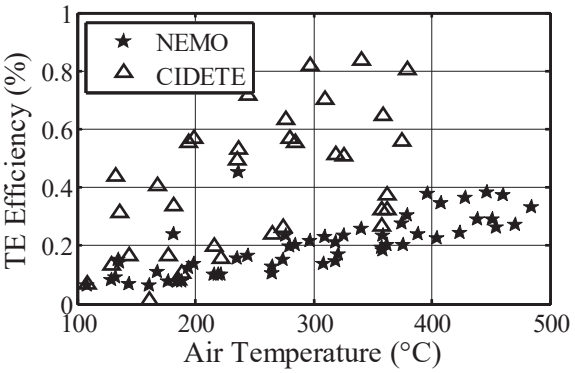

Fig. 12 $Si_{80}Ge_{20}$ *vs.* Bi_2Te_3: inlet air temperature (°C) vs. TEM TE efficiency (%)

The conversion efficiency was determined by combining test results and an estimate calculation. Since it was not possible with our current test configuration to measure the heat evacuated by each TEM, the heat evacuated through the TEG was calculated by using the measured temperatures on the inlet and outlet of the single tube heat exchanger and by applying (8):

$$P_{th} = Q_{air} \times Cp_{air} \times (T_{ea} - T_{sa}) \quad (8)$$

This evacuated heat includes also the heat flux emitted from the cold blocks and heat loss by radiation. Considering the last two to be relatively negligible, we assume that the entire heat is evacuated through the TEM. Hence, the conversion efficiency is then calculated by using (9):

$$\eta = P_{elec} / P_{th} \quad (9)$$

Fig. 12 shows the conversion efficiency of the TEG with each Bi_2Te_3 and $Si_{80}Ge_{20}$ TEM. Since no measurement has been made for the 4 TEM charged with exactly the same load resistance, the generated power of a single TEM was multiplied by 4 to represent the generated electrical power of the TEG. The TEG conversion efficiency reached around a maximum of 1%, using Bi_2Te_3 TEM and around 0.5 % using $Si_{80}Ge_{20}$ TEM. The lower performance of the $Si_{80}Ge_{20}$ TEM is justified since the optimum operating range of these modules is 400-800 °C, and the temperature range during our tests was 108-468 °C. Moreover, the conversion efficiency is relatively low for both types of modules since it is calculated assuming that all the heat is evacuated through the TEM, knowing that the TEMs fill only 13% of the available heat exchange surface. So, covering the available surface of the heat exchanger with more TEMs may give higher conversion efficiency. Fig. 12 does not show any clear trend for the conversion efficiency of the TEG according to inlet air temperature variation, since all operating points were measured with different flow rates, which affect eventually the heat transferred through the heat exchanger and the conversion efficiency. Hence, it is globally seen in the Fig. 12 that conversion efficiency increases with the air inlet temperature and that it is higher while using the CIDETE TEM then when using NEMO TEM, which is consistent with literature [28].

For possible marine engine application, the pressure losses through the heat exchanger have been measured and evaluated. Pressure losses of 30 mbar are considered as the maximum acceptable value for any energy recovery system installed on marine engine exhaust since high pressure losses result in an increase of fuel consumption and even engine malfunction beyond 60 mbar [22]. Fig. 13 shows the pressure drop through the single tube heat exchanger. Two pressure measuring sensors were installed on the inlet and the outlet of the heat exchanger to measure the pressure losses. It reached a maximum of 1.7 bars for a flow rate of 40.5 g/s with air temperature around 362 °C and a minimum of 237 mbar for a hot gas temperature of 108 °C. It must be noted that a sonic nozzle is noticed for air flow rate higher than 44 g/s. Such high pressure drop is clearly indicated that the current TEG is undersized for the diesel engine application targeted in this study.

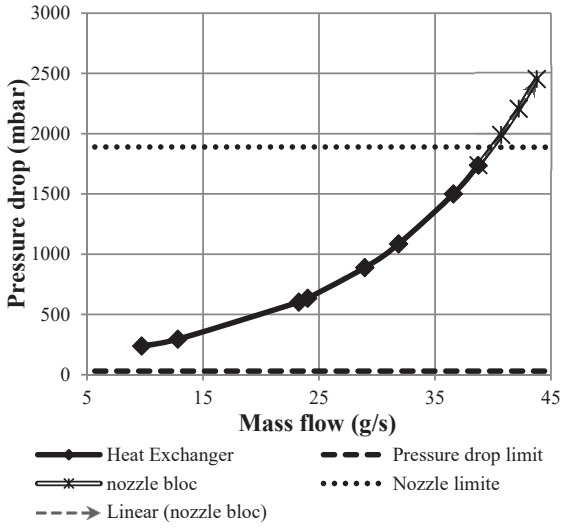

Fig. 13 TEG device pressure drop

V. Conclusion

This tests campaign allowed characterizing the TEG on 36 engine operating points using the Bi_2Te_3 TEM from CIDETE Ingenieros SL and 56 operating points for the Si80Ge20 TEM from HBOB SAS. The tests aimed at comparing the performance of the TEM on engine operating points and at studying the possibility of the application of these TEM and this TEG to a real marine Diesel engine.

The results showed a higher performance (power and conversion efficiency) of the Bi_2Te_3 TEM compared to the $Si_{80}Ge_{20}$ TEM, on same operating points. The possibility of integrating these Bi_2Te_3 TEM on a marine Diesel engine is uncertain because they are not designed to support temperature higher than 207 °C, which is relatively low for exhaust gas temperature. However, finding other commercial Bi_2Te_3 TEM which supports higher temperatures will be interesting for completing this study. The $Si_{80}Ge_{20}$ TEM showed remarkable performance stability and durability on all engine operating points. However, most of operating points were outside their optimum operating range, giving low conversion efficiency. Hence, their single use is certainly nonproductive for a Diesel engine application.

The possibility of the combination of these two TEMs for a better performance and wide application have been also studied. While using $Si_{80}Ge_{20}$ TEM on the inlet air side of the heat exchanger (where we have the highest temperatures) and Bi_2Te_3 TEM on the air outlet side of the heat exchanger is a good idea, it was not relevant for this heat exchanger since the results showed that the temperature difference between the inlet and the outlet end of the heat exchanger is not more than 10 °C. So, a longer tube heat exchanger is needed for this type of application. Furthermore, the too high pressure drop measured on this TEG, indicates that a redesign is needed to

fit better with the engine exhaust conditions (flow rates).

ACKNOWLEDGMENT

The work in this article is done in a joined research program between CEA Tech and Ecole Centrale de Nantes. The authors want also to thank the "Region des Pays de la Loire", in France, for their financial contribution to this study.

REFERENCES

[1] C. Yu and K. T. Chau, "Thermoelectric automotive waste heat energy recovery using maximum power point tracking," Energy Convers. Manag., vol. 50, no. 6, pp. 1506–1512, juin 2009.
[2] Y. Y. Hsiao, W. C. Chang, and S. L. Chen, "A mathematic model of thermoelectric module with applications on waste heat recovery from automobile engine," Energy, vol. 35, no. 3, pp. 1447–1454, Mar. 2010.
[3] "Exhaust Heat Recovery using Electro-Turbogenerators." (Online). Available: http://papers.sae.org/2009-01-1604/.
[4] "Heat Recovery and Bottoming Cycles for SI and CI Engines - A Perspective." (Online). Available: http://papers.sae.org/2006-01-0662/.
[5] L. T. N Espinosa, "Rankine cycle for waste heat recovery on commercial trucks: approach, constraints and modelling."
[6] "Turbocharger Modeling for Automotive Control Applications." (Online). Available: http://papers.sae.org/1999-01-0908/.
[7] "The Potential for Thermo-Electric Devices in Passenger Vehicle Applications." (Online). Available: http://papers.sae.org/2010-01-0833/.
[8] "Simulation of Fuel Economy Effectiveness of Exhaust Heat Recovery System Using Thermoelectric Generator in a Series Hybrid." (Online). Available: http://papers.sae.org/2011-01-1335/.
[9] S. LeBlanc, "Thermoelectric generators: Linking material properties and systems engineering for waste heat recovery applications," Sustain. Mater. Technol., vol. 1–2, pp. 26–35, Dec. 2014.
[10] "Thermoelectrics Handbook: Macro to Nano," CRC Press, 09-Dec-2005. (Online). Available: https://www.crcpress.com/Thermoelectrics-Handbook-Macro-to-Nano/Rowe/9780849322648.
[11] "Waste heat recovery device."
[12] "A Review On Thermoelectric Generator: Waste Heat Recovery from Engine Exhaust." (Online). Available: https://www.researchgate.net/publication/282850933_A_Review_On_Thermoelectric_Generator_Waste_Heat_Recovery_From_Engine_Exhaust.
[13] J. LaGrandeur, D. Crane, S. Hung, B. Mazar, and A. Eder, "Automotive Waste Heat Conversion to Electric Power using Skutterudite, TAGS, PbTe and BiTe," in 2006 25th International Conference on Thermoelectrics, 2006, pp. 343–348.
[14] L. E. Bell and D. T. Crane, "Thermoelectric power generator for variable thermal power source," US9006556 B2, 14-Apr-2015.
[15] X. Zhang, K. T. Chau, and C. C. Chan, "Overview of Thermoelectric Generation for Hybrid Vehicles," J. Asian Electr. Veh., vol. 6, no. 2, pp. 1119–1124, 2008.
[16] C. Yu and K. T. Chau, "Thermoelectric automotive waste heat energy recovery using maximum power point tracking," Energy Convers. Manag., vol. 50, no. 6, pp. 1506–1512, juin 2009.
[17] C.-T. Hsu, G.-Y. Huang, H.-S. Chu, B. Yu, and D.-J. Yao, "Experiments and simulations on low-temperature waste heat harvesting system by thermoelectric power generators," Appl. Energy, vol. 88, no. 4, pp. 1291–1297, avril 2011.
[18] S. Kim, S. Park, S. Kim, and S.-H. Rhi, "A Thermoelectric Generator Using Engine Coolant for Light-Duty Internal Combustion Engine-Powered Vehicles," J. Electron. Mater., vol. 40, no. 5, pp. 812–816, Mar. 2011.
[19] F. Frobenius, G. Gaiser, U. Rusche, and B. Weller, "Thermoelectric Generators for the Integration into Automotive Exhaust Systems for Passenger Cars and Commercial Vehicles," J. Electron. Mater., vol. 45, no. 3, pp. 1433–1440, Mar. 2016.
[20] E. F. Thacher, B. T. Helenbrook, M. A. Karri, and C. J. Richter, "Testing of an automobile exhaust thermoelectric generator in a light truck," Proc. Inst. Mech. Eng. Part J. Automob. Eng., vol. 221, no. 1, pp. 95–107, Jan. 2007.
[21] L. Huang, Q. Zhang, B. Yuan, X. Lai, X. Yan, and Z. Ren, "Recent progress in half-Heusler thermoelectric materials," Mater. Res. Bull., vol. 76, pp. 107–112, avril 2016.
[22] "MAN Diesel and Turbo - About us." (Online). Available: http://dieselturbo.man.eu/company/about-us. (Accessed: 18-May-2016).
[23] "Slow Steaming in Container Shipping." (Online). Available: https://www.researchgate.net/publication/254051395_Slow_Steaming_in_Container_Shipping.
[24] K. Romanjek, S. Vesin, L. Aixala, T. Baffie, G. Bernard-Granger, and J. Dufourcq, "High-Performance Silicon–Germanium-Based Thermoelectric Modules for Gas Exhaust Energy Scavenging," J. Electron. Mater., vol. 44, no. 6, pp. 2192–2202, Jun. 2015.
[25] A. Lahwal, "Thermoelectric Properties of Silicon Germanium: An Investigation of the Reduction of Lattice Thermal Conductivity and Enhancement of Power Factor," Diss., May 2015.
[26] "Thermoélectricité : des principes aux applications | Techniques de l'Ingénieur." (Online). Available: http://www.techniques-ingenieur.fr/base-documentaire/sciences-fondamentales-th8/proprietes-electriques-et-electrochimiques-42336210/thermoelectricite-des-principes-aux-applications-k730/.
[27] "Thermoelectric Modules." (Online). Available: http://www.termo-gen.com/pages/modules.html.
[28] N. Espinosa, "Contribution to the study of waste heat recovery systems on commercial truck diesel engines," Thèse de doctorat, Institut national polytechnique de Lorraine, France, 2011.

A. Nour Eddine born in Lebanon on March, 3, 1989. Nour Eddine has a bachelor degree in mechanical engineering from the Lebanese University, Beirut, Lebanon. A master's degree in automotive engineering from Politecnico di Torino, Turin, Italy. A master's degree in energy and propulsion system's from the Ecole Central de Nantes, Nantes, France.

He worked as a Mechanical Engineer in Mechanical and industrial technologies co. and as a Project Coordinator with touch engineering co. in Lebanon. He made the automotive engineering master's training with Fiat power train in Turin, Italy, and the energy and propulsion master's training at the ecole central de Nantes in Nantes, France. He currently holds the position of research engineer and PhD student in the commissariat d'energies atomiques et alternatives (CEA). The job location is CEA Tech Pays de la Loire, Technocampus Océan, 5 Rue de l'Halbrane, 44340 Bouguenais, France.

PhD student Nour Eddine is a member of American Society of Heating, Refrigeration and Air conditioning (ASHREA) since 2011 and a member of Associazione Tecnica del Automobile (ATA) since 2013.